Action Potential Classification with Dual Channel Intrafascicular Electrodes

Timothy G. McNaughton, *Student Member, IEEE,* and Kenneth W. Horch, *Member, IEEE*

***Abstract*—Using recordings of peripheral nerve activity made with carbon fiber intrafascicular electrodes, we compared the performance of three different recording techniques (single channel, differential, and dual channel) and four different unit classification methods (linear discriminant analysis, template matching, a novel time amplitude windowing technique, and neural networks) in terms of errors in waveform classification and artifact rejection. Dual channel recording provided uniformly superior unit separability, neural networks gave the lowest classification error rates, and template matching had the best artifact rejection performance.**

I. Introduction

INTRAFASCICULAR electrodes record neural activity from small groups of axons (single units) within individual fascicles of peripheral nerves. Because the axons supply varied sensory modalities and receptive fields, full utilization of the information contained in these multiunit recordings requires discriminating the individual activity patterns of single units within the recording. Each single unit that can be reliably tracked represents an independent channel of high resolution somatosensory or motor information. A sufficient number of such channels could supply information regarding joint position, skin indentation, muscle length and tension, etc., that would be useful in functional electrical stimulation systems intended to restore functional mobility to victims of paralysis due to central nervous system trauma.

Discrimination of single unit activity in recordings made with single channel intrafascicular electrodes implanted in feline peripheral nerves has been shown to provide information sufficient for distinguishing between different types of sensory stimuli [1]. However, the limited number of units that could be uniquely identified with this electrode configuration and discrimination technique make this system less attractive than desired. The goal of the work described here was to improve the average yield of separable units in order to maximize the number of independent channels of information available from each intrafascicular implant.

The task of discriminating single unit activity in multiunit recordings is a pattern classification problem that has generated considerable interest [2], [3]. Acceptable techniques for neuroprosthetic applications must perform in real-time and achieve high classification rates while exhibiting good rejection of noise due to motion, electromyographic activity, and other artifacts. All spike sorting algorithms rely on differences in the shapes of the extracellularly recorded action potentials from the different units in the recorded population. These differences arise partly because of differences in the relative positions of the source cells with respect to the electrode. Dual channel "stereotrodes," which take advantage of this sensitivity of the wave shape to electrode position, have significantly improved the classifiability of neurons in the central nervous system by recording activity from two different locations, thereby delivering additional wave shape information [4].

For the present study, we developed a dual channel intrafascicular electrode for use in peripheral nerves and compared its performance to that of single channel electrodes for delivering information suitable for classifying action potential waveforms. We also evaluated the usefulness of several different classification techniques at the tasks of waveform classification and rejection of artifacts as applied to recordings made with these electrodes. Four techniques were studied: linear discriminant analysis, a variation of principal component analysis [2]; template matching, an optimal Bayesian classifier [5]; a novel variation of time amplitude windowing method that performs significantly better than classical windowing techniques [6]; and neural network classification, which has yielded promising results in preliminary studies in our lab [7].

II. Methods

A. Electrode Design and Fabrication

Lengths of untwisted carbon fiber yarn (Thornel® 650/42, Amoco, Greenville, SC) comprised of single fibers 5.1 μm in diameter were repeatedly subdivided to yield bundles tapering from approximately 300 fibers to approximately 30 fibers. The distal 2.5 cm of each bundle was then subdivided and trimmed under magnification until eight single fibers remained. The resultant multistrand electrode was insulated by electrochemical deposition of 1–2 μm of polyphenylene oxide [8]. The electrode recording zone was prepared by exposing 1 mm of the bundle's shaft at a point 1.5 cm back from the tip by vaporizing the insulation within a heated platinum loop. The impedance of the electrode at 1 kHz in saline was 5–10 kΩ. No activation step was necessary to achieve noise levels comparable to those of Pt-Ir intrafascicular electrodes (7 μV p-p at 0.3–5 kHz).

The completed dual channel electrode consisted of a trio of impedance-matched single electrodes, two affixed to a 50 μm tungsten wire needle with cyanoacrylate and the third for use as an extrafascicular reference.

Manuscript received February 26, 1993; revised March 7, 1994. This work was supported by a grant from the NINDS of NIH.

The authors are with the Department of Bioengineering, University of Utah, Salt Lake City, UT 84112 USA.

IEEE Log Number 9402016.

0018-9294/94$04.00

B. Animal Preparation

The technique for implanting intrafascicular electrodes in cat radial nerve has been described previously [9], [10]. Briefly, the nerve was exposed near the elbow and the tungsten needle threaded for approximately 1 cm along the inside of a single fascicle and used to pull the rest of the electrode through, centering the recording zones longitudinally in the fascicle. After implantation, the needle was cut off, and the longitudinal distance between the recording zones of the two intrafascicular electrodes adjusted to maximize their differential signal. This distance was always between one and four mm. The reference electrode was placed outside the fascicle adjacent to the intrafascicular pair. The electrode was anchored to the perineurium with sutures at both the distal exit and proximal entry point and the wound was closed. Ten dual channel electrodes were implanted in acute experiments involving six cats. Anesthesia was maintained with sodium pentobarbital administered intravenously throughout the implantation and subsequent recording periods. At the end of the experiment, the animal was euthanized with an overdose of anesthetic.

C. Neural Activity Recording and Data Collection

The radial nerve is a pure sensory nerve comprised of axons which innervate mechanoreceptors on the foreleg and paw. Single mechanoreceptor units were located by probing the skin or individual hairs with a hand-held blunt rod or brush and then activated in a phase-locked fashion with a tunable vibrating probe [10]. Units were activated and phase-locked to the stimulus for one to five minutes at frequencies between 10 and 200 Hz. Several thousand action potentials were recorded from each unit. Care was taken to ensure that all units with action potentials greater than approximately 1.5 times the background noise level were recorded from.

Three different recording configurations were used. In the first, *single channel* signals from one of the intrafascicular electrodes were recorded with reference to the extrafascicular electrode. In the second, a *differential* recording was made between the intrafascicular pair of electrodes, and in the third, *dual channel* recordings were made by recording the two single channels simultaneously. The signals were amplified, band-pass filtered (0.3–5 kHz) and recorded for off-line analysis. For the single channel and differential configurations, action potentials were digitized (30 μs sampling interval, 12 bit A/D) and aligned so their peaks were centered in the 32 points stored for each waveform. Dual channel data was collected by alternately digitizing the two single channels every 15 μs so that each was sampled every 30 μs. The waveforms in the dual channel configuration were peak centered with reference only to the channel in which the action potential was larger, so that the temporal relationship between the two channels was preserved. The 32 samples from each channel were then appended and stored as a 64 sample waveform.

This experimental design enabled us to collect a large number of examples of action potential waveforms whose source unit was known. Therefore, no clustering step was needed to preprocess the data. The variables employed in the classification techniques were simply the raw digitized waveform points. In a previous study, we showed that frequency domain (FFT) and time domain (peak height, rise/fall time) features were not as good as point features for classification, and point features have the advantage that no additional processing is required after the digitization [6].

For each unit, a set of 1 000 action potentials was culled from the digitized data solely on the basis of peristimulus latency. Test sets of 200 action potentials were selected at random from these sets with the remaining waveforms forming the training sets. For each of the four pattern classification techniques described below, only training set data was used to compute or learn the parameters used in the discrimination functions. The performance of each was evaluated with action potentials from the test sets.

D. Linear Discriminant Analysis

Linear discriminant analysis is a variation of principal component analysis in which the components, linear combinations of the data points, are selected which optimize the linear separation of the data clusters. Linear discriminant analysis is available as a standard function in commercially available statistical software such as SPSS®, so it represents a useful way to benchmark pattern classification studies. In this study, we performed linear discriminant analysis using both Euclidean and Mahalanobis' distance metrics to select factors. Mahalanobis' distance corrects for unequal variances at the different waveform points and for autocorrelations in the noise [11]. Additionally, for the Euclidean analyses, three different tolerance levels were selected which resulted in discriminant functions which retained 100%, 50%, and 25% of the waveform points in the factors. Using all the points produced the best results, so the data presented below are from analyses that included all the data points.

E. Time-Amplitude Windowing

Previous work in our lab employed a time-amplitude window discriminator for classification [6]. This is a widely used classification method popular because of its relative simplicity. For a unit to be separable with a window discriminator, some portion of its waveform must be completely distinct from the corresponding portion of the waveforms of all other units in the recorded population. We have developed a slightly more sophisticated method which uses time-amplitude windows to classify units into smaller and smaller subsets, which are then subdivided until individual units remain. This binary tree clustering technique requires only that at each step a given unit be sufficiently discriminable at some point along its waveform from at least one other unit in the subset. In the previous study, an action potential was assigned to all the units whose windows it fit [6]. In the present study, an action potential was assigned to the first unit whose windows it matched. This was done to facilitate comparison to the other techniques, which made unique assignments of action potentials.

F. Template Matching

In template matching, a mean waveform with pointwise variances is computed for each unit to be discriminated.

Classification then entails matching each action potential to the closest of these templates using some kind of distance metric. The theoretically optimal Bayesian method uses Mahalanobis' distance [11]. We performed template matching using both Euclidean and Mahalanobis' distances and also investigated the effect of training set size on the performance of these methods. In using this method, an action potential was assigned to the unit to which it came closest, except when artifact rejection was needed. In the latter case, a further constraint was placed on the distance as described below.

G. Neural Networks

We trained three-layer, fully connected, feedforward networks with back propagation of error to perform the waveform classification [7], [12]. We compared the performance of two different network architectures. The first was a standard monolithic architecture that involved a single network with as many output nodes as there were units to be classified. The second used a distributed architecture that consisted of a collection of separate neural networks, one for each unit. Each network was trained to discriminate one of the units from the rest. Modified batch training was used in which the network weights were updated only after action potential waveforms from each of the units had been presented to the network. To aid convergence in the distributed networks, the effect of the target unit of interest was weighted to balance the sum of the effects of the other, nontarget units. The update coefficients used in both architectures were: learning, 0.9; momentum, 0.6. Each network was trained several times, and training was continued with periodic cross-validation until the system error no longer improved. Training took less than 10 minutes on an IBM RS/6000.

In use, an action potential was assigned to the unit corresponding to the node having the highest value (for the monolithic network) or to the unit whose network had the highest output value, except when it was desired to discriminate against artifacts [7]. In the latter case, a further constraint was provided, as described below.

H. Artifact Rejection

Most real world classification problems are not restricted to simply finding the closest match of an input element to a restricted group of templates or clusters. Real world inputs include artifactual waveforms which should not be matched to any of the groups. Artifacts can arise from noise sources not directly related to the neural activity of interest, such as electromyographic activity or electrode motion, superposition of action potentials from two or more units, and activity of units not identified in the training process. The first two give rise to waveforms that are very different in shape from a typical action potential, and, thus, are fairly easy to recognize as artifacts. Recognition of the third type of artifact is much more difficult, so we focused on it.

To evaluate the susceptibility of the classification methods to corruption by activity in units not in the training set, we combined units from multiple recordings to form collections of 16 units which we knew to be fully discriminable by each of the classification methods. We then formed sets of "real" units to be classified and "artifactual" units to be rejected by randomly dividing these collections into halves. Action potentials from the "real" units were used for training the classifiers, and both "real" and "artifactual" units were used for testing classification performance.

For the neural network method, when presented a waveform from a unit for which a network has been trained, the value of the network's corresponding output node should approach unity and all other nodes should be close to zero. When artifactual input is presented, all outputs should be low. We compared two methods for improving artifact rejection by the neural networks. In the first, the maximum node had to exceed an absolute threshold. In the second, the values of the maximum node and the next maximum node were required to differ by a threshold criterion. If, for any waveform, the network output failed to meet or exceed the acceptance criterion, the waveform was rejected and not assigned to any unit.

A similar process was used for the template matching technique except that the threshold criterion for each unit was based on the statistics of the observed distances of the waveforms of a unit to that unit's template.

III. Results

A. Dual Channel Recordings

Fig. 1 shows averaged waveforms of action potentials from four readily separable units in a dual-channel recording. The longitudinal displacement between the two recording sites was 3 mm. The figure illustrates the general similarity of action potential waveforms recorded extracellularly with intrafascicular electrodes. Because the two channels are digitized simultaneously, the figure also illustrates how temporal, as well as wave shape, information is preserved in the two channels. The action potentials are centered relative to the peak point in the channel in which they are largest. The three units that were larger in channel A (upper trace) than in channel B (lower trace) were peak aligned in channel A, and their waveform peaks in channel B are delayed by an amount corresponding to their respective conduction latencies. The fourth unit was peak aligned in channel B, so its peak appears advanced in channel A relative to the other three units.

An average of 8.7 units (standard error of ± 0.75 units) was present in each of the recordings made from the 10 implants used in this study. Like the data illustrated in Fig. 1, units were usually, but not always, present in both channels and had similar shapes, but different amplitudes, in the two channels.

B. Training Set Requirements

The number of waveforms used as exemplars to train a pattern classification method must be sufficiently high so that the performance of the method with new data is not significantly different from its performance with training data. Classification results for the windowing method, neural networks, linear discriminant analysis and template matching with Euclidean distance indicated that these methods gener-

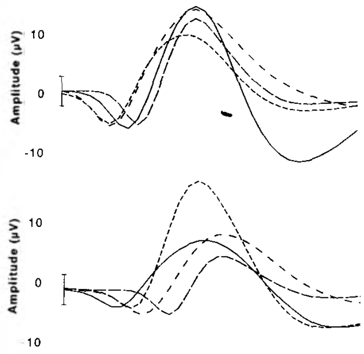

Fig. 1. Averaged waveforms of action potentials from four different units present in a typical recording made with dual channel intrafascicular electrodes. The upper traces show the waveforms as recorded from channel A of the electrode, the lower traces show the potentials as they appeared in channel B. Each unit is indicated by a different line style, which is the same for the two traces. The averaging was performed on digitized data sampled at 30 μs intervals. Pooled standard deviation is indicated at the first digitized point in each channel. The trace duration is 930 μs. Peak-to-peak noise in these recordings was approximately 7 μV.

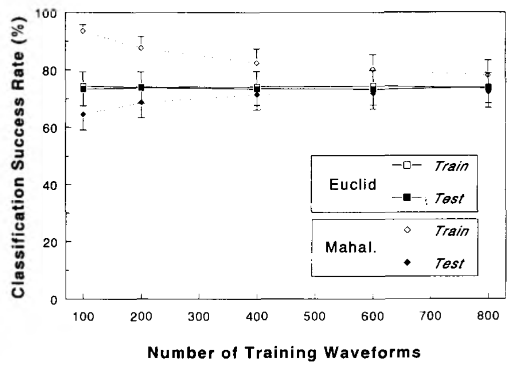

Fig. 2. Influence of the number of action potential waveforms in the training set used to create templates on classification performance of the template matching technique using two different distance metrics. Classification success is the fraction of action potentials correctly assigned to their source unit by the classifier, under conditions in which each unit contributed equally to the population of action potentials to be classified. Data from single channel and dual channel recordings have been pooled. Train—classification results when testing was done with the same waveforms used to build the classification templates. Test—performance with wave forms not included in the training set. Euclid—template matching with Euclidean distance. Mahal.—Template matching with Mahalanobis' distance. Each point shows mean ± standard error (error bars are restricted to one side of the data points for clarity) with $N = 20$.

alized well with training sets of a few hundred waveforms for each unit. However, both template matching and linear discriminant analysis using Mahalanobis' distance showed strong dependence on training set size. This is illustrated in Fig. 2 for template matching. Using Euclidean distance, the discrimination performance on the test data set was similar to the performance on the training set, irrespective of training set size. But, for the same sets of waveforms classified using Mahalanobis' distance, there was a strong dependence on the number of action potential waveforms in the training set. For small training sets, action potentials from the training set were classified extremely well, but performance with test set data was poor. As the training set size increased, the performance with both sets converged toward the performance obtained with Euclidean distance. Complete convergence would have required training sets larger than our data sets.

For the classification results described below, we used Euclidean distance for both template matching and linear discriminant analysis.

C. Network Structure

The degree of complexity of classification problems which can be solved by a given neural network depends, in part, upon the number of hidden layer nodes in the network architecture. Because unnecessary nodes result in unnecessary computation, it is important, for applications requiring real-time operation, to determine the minimum necessary number of nodes. We evaluated how classification rate was affected as the number of hidden layer nodes was varied in both monolithic and distributed neural networks for both single channel and dual channel recordings.

The results are presented in Fig. 3. The classification rates of both monolithic and distributed architectures were not different, provided the networks were adequately sized. However, the distributed networks required only about two hidden nodes to achieve their full classification rate whereas the monolithic networks required about five hidden layer nodes. Similar results were obtained for both dual channel data (64 input nodes) and single channel data (32 input nodes). Note that both types of networks performed better with dual channel data than with single channel data.

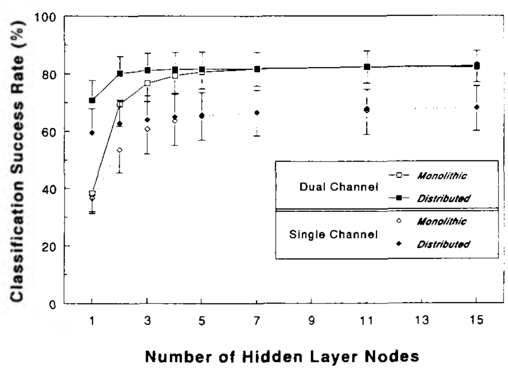

Fig. 3. Influence of neural network complexity in terms of number of nodes in the hidden layer on the classification performance of three-layer neural networks organized in two different architectures. Classification success is defined as described in Fig. 2. Monolithic: a single network is trained to discriminate all units in a given recording. The number of output nodes is the same as the number of units to be classified. Distributed: individual networks are each trained to recognize just one of the units in the recording. Performance curves with both single channel and dual channel recording methods are shown. Each point shows mean ± standard error (error bars are restricted to one side of the data points for clarity) with $N = 10$.

D. Recording Mode and Classification Technique

In quantifying the performance of the recording techniques and classification methods, we wanted to avoid making an

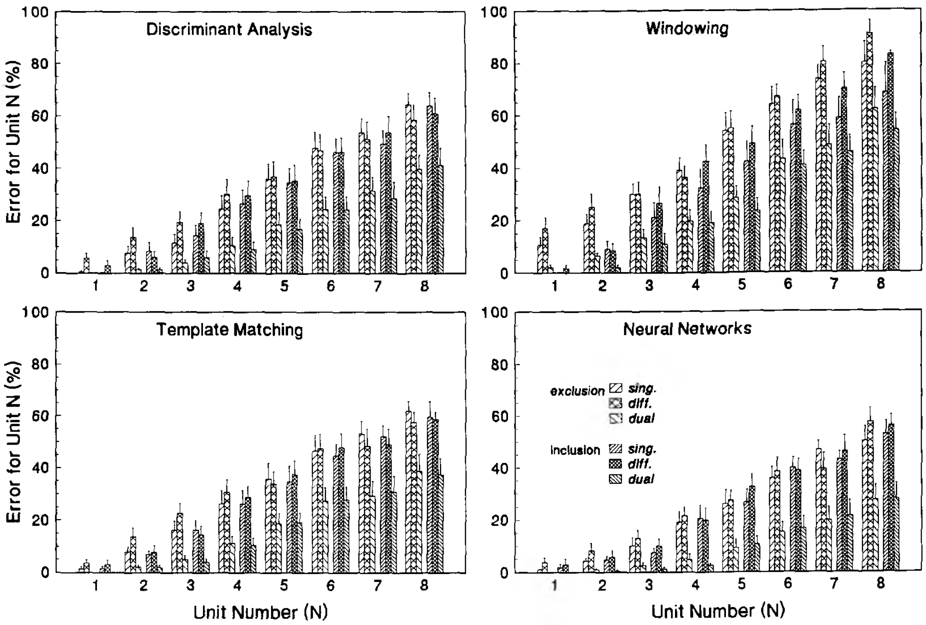

Fig. 4. Classification error rates for units in multiunit recordings as a function of recording method and classification method. The three recording methods were: single channel, differential, and dual channel. The classification methods were: linear discriminant analysis, time/amplitude windowing, template matching and neural networks. Two types of errors are shown (as mean ± standard error): exclusion, the fraction of action potentials originating from a given unit not assigned to that unit, and inclusion, the fraction of action potentials assigned to a unit not originating from that unit. The units were ordered separately for each error type. Acceptance criteria were relaxed, minimizing exclusion error at the cost of maximizing inclusion errors. Data has been pooled from 10 implants.

arbitrary assumption about what constitutes good performance. Therefore, the data are presented in terms of the types and rates of errors observed in classifying individual unit potentials in the recordings. Two types of errors were measured: exclusion and inclusion. An exclusion error occurred when an action potential originating from a given unit was not assigned to that unit (e.g., an action potenital from unit n was assigned to some other unit or was rejected as an artifact). An inclusion error occurred when an action potential was assigned to a unit other than its actual source (e.g., an action potential from unit m was assigned to unit n). The units in each recording were ranked from "best" to "worst" on the basis of error rate, and the data for units of corresponding rank were averaged between experiments. The sorting was done independently for each type of error, so, the order of units in general was not the same for the two types of errors. However, there was a positive correlation between error rates among the units: those having low exclusion error rates tended to have low inclusion errors as well.

The panels in Fig. 4 show error rates for the different classification techniques (linear discriminant analysis, windows, templates, and neural networks) grouped according to recording method (single, differential, and dual channel) and type of error. The data in Fig. 4 are based on classification without artifact rejection constraints. This minimizes exclusion error (action potentials tend to be assigned to the closest unit without regard to the certainty of the assignment), but maximizes inclusion error (almost no action potentials are rejected as artifacts). The effect of applying artifact constraints is presented in the next section below.

The data in Fig. 4 demonstrate that for each classification method, dual channel recording was superior to single channel or differential recording. Dual channel recording reduced the error rate relative to single channel recording by 61% for discriminant analysis, 48% for windowing, 59% for template matching, and 70% for neural network processing.

The performance of the classification methods, from best to worse was: neural networks, templates, linear discriminant analysis, and windows. The template matching and linear discriminant analysis methods performed quite similarly, whereas the neural network approach was uniformly better than any of the other three methods. Fig. 5 directly compares template and neural network classification results from dual channel recordings. With the neural network method, up to five units could be classified with inclusion and exclusion error rates at or below 10%.

E. Artifact Rejection

To compare the performance of windows, templates and neural networks at rejecting artifactual waveforms, we computed the inclusion error rate for action potential waveforms drawn from a set of units to which the systems had not been trained. This was done for different values of the acceptance criteria described in Section II, and the results were expressed in terms of the success rate at which test action potentials from units in the training set were correctly assigned to their sources. This represents a "worst case scenario" for artifact effects. All the methods would work well in rejecting artifacts that do not resemble action potentials. We wished to examine

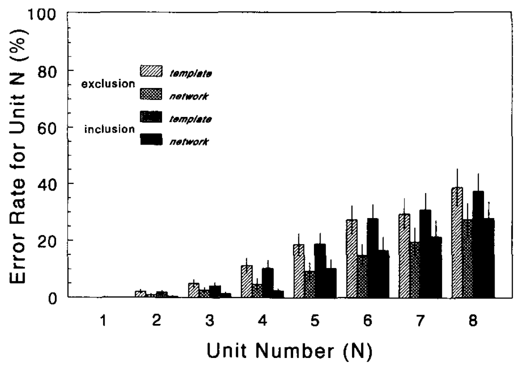

Fig. 5. Dual channel recording classification error rates for template matching and neural networks. The data are taken from Fig. 4 and have been replotted to facilitate comparison between classification methods.

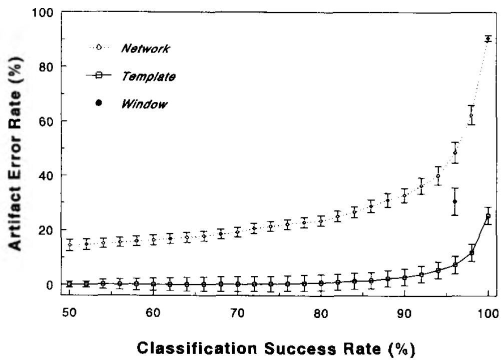

Fig. 6. Rate of erroneous inclusion of artifactual waveforms as a function of classification success rate for three different pattern classification techniques. Classification success rate, as defined in Fig. 2, was controlled by changing the acceptance criteria for the classifiers as described in Section II. Right-most points of these curves were obtained by performing classification with completely relaxed acceptance criteria. With more stringent acceptance criteria, more artifacts are rejected but the classification rate for real waveforms falls off as well. Shown are means ± standard errors with $N = 10$.

here their performance with artifacts that would normally be very difficult to discriminate against.

The results are shown in Fig. 6. For the windows, a fixed criterion (implicit in setting the limits for the windows) was used. For the templates and neural networks, error rate increased as the criterion for acceptance was lowered to allow inclusion of more of the actual action potentials coming from the units in the data set. More stringent requirements for acceptance of a classification decision resulted in a decreased rate of inclusion of artifacts, at the cost of a reduced classification rate for real data. The template method performed best at rejecting artifacts at all levels of classification success rate.

The data in Fig. 6 are related to the data in Figs. 4 and 5 in the following way. Classification success rate is (1—exclusion error rate), so a classification success rate of 100% corresponds to an exclusion error rate of 0% (all the action potentials are assigned to the correct unit), a success rate of 95% corresponds to an exclusion error rate of 5% (since this fraction of action potentials was not assigned to the source unit), etc. To increase the success rate (decrease exclusion error rate), the classification criteria are made less strict. This increases both artifact errors (i.e., assignment of signals not originating from units in the training set) and inclusion errors (assignment of action potentials to the wrong unit). The curves in Fig. 6 can be used to approximate the effect of how exclusion and inclusion error rates in Figs. 4 and 5 would change with different acceptance criteria. The data in those figures represents the behavior of the systems near the rightmost end of the curves in Fig. 6.

IV. Discussion

The additional information regarding action potential wave shape provided by dual channel electrodes decreased errors in discriminating single units by up to 70% over single channel recording. The surgical implantation procedure for dual electrodes is identical to that for single electrodes because both electrodes are inserted simultaneously with the same needle. Therefore, the advantages of dual channel recording are gained for negligible additional effort.

Single wire electrodes have been previously shown to be well tolerated on a chronic basis [9]. Because the dual electrode is smaller and more flexible than single 25 μm Pt-Ir wires, dual electrodes should cause no more tissue trauma than single channel electrodes upon implantation. The mechanical properties of carbon fiber, which include excellent fatigue life, tensile strength and biocompatibility, should make it an appropriate material for use in chronically implanted intrafascicular electrodes [13], [14]. The multistrand geometry both increases the recording surface area, resulting in lower impedance and lower noise, and increases flexibility, compared to the single wire geometry. There is no apparent difference in the inherent noise level of these carbon fiber electrodes as compared to Pt-Ir electrodes, even though the bulk conductivity of carbon fiber is significantly less than that of platinum.

Although the binary search windowing technique performed better than our previous windowing technique [6], it performed worse than the other three techniques used in this study. However, it has the advantages of simple implementation and very fast classification speed compared to the other methods. No floating point operations and, on average, only $2N$ integer comparisons are required for classification among N units, making it much less computationally complex than the other methods.

Using action potential waveforms with simulated noise, Bankman has shown that, under certain conditions, template matching with the Mahalanobis metric can improve classifiability over Euclidean template matching [5]. Mahalanobis' distance is computed with the inverse of the covariance matrix formed from each group of training set action potentials. We found that constructing covariance matrices that accurately reflected the distribution and autocorrelation of the noise in our test sets required relatively large training sets in both linear discriminant analysis and template matching. Optimal template matching with the Mahalanobis' distance assumes that the distributions of the data form hyperelliptical clusters. A further assumption for a minimum distance Mahalanobis classifier is that the covariance matrices for all of the classes are identical, that is, the hyperellipses are of equal size, shape and orientation. A minimum distance Euclidean distance classifier assumes simpler, hyperspherical clusters. The observation that the results obtained using Mahalanobis' distance with adequately sized training sets converge to those obtained with Euclidean distance imply a fairly simple spherical clustering of the data. For our application, the additional computational complexity required by Mahalanobis' method is unnecessary.

Irrespective of the nature of the distributions within the clusters, the sensitivity of the Mahalanobis method to training set size was initially unexpected. The explanation for this effect may lie with the source of noise in real, as distinct from simulated, data. There are two types of noise in our data: source noise and phase noise. The source noise is basically band-pass filtered $1/f$ noise derived from physical processes associated with the recording of extracellular activity in peripheral nerves [15]. The phase noise derives from the asynchronicity between the digitization process and the production of action potentials. This means that digitally aligned action potentials do not provide physically aligned source potentials. Given the limited signal-to-noise ratios characteristic of these signals, the misregistration can easily exceed the sampling period of the digitizer (30 μs in the present experiments). Unlike source noise, which is essentially constant and symmetrically distributed at each point on the waveform (changes in membrane impedance of the axons associated with passage of an action potential do not affect source noise for externally recorded signals), the amplitude of phase noise depends on the slope (first derivative) of the waveform and, since the second derivative of the waveform is generally nonzero, the distribution of the phase noise is not symmetrical.

As a result, while each digitized action potential provides 32 samples of source noise, a single action potential provides only a single sample of phase noise at each point. Small training sets do not provide adequate population samples of the phase noise, but can provide adequate samples of the source noise. It is not surprising, then, that a method which is sensitive to the fine details of noise distribution, such as using Mahalanobis' distance, will give good results on a limited training set when tested with the same data, but will fail when presented with novel test data. Only with large training sets will the true magnitude of the contribution from phase noise be apparent, and performance will fall on the training set and rise on the test set.

Is it worth developing a method which determines and uses the distribution of the source and phase noise on a point-by-point basis? We suggest, without proof, that the answer is no. The similarity in performance of the linear discriminant analysis, template and neural network methods implies that the limitations in classifying action potential sources in these recordings stem from the similarity of the potentials from different units and the limited signal-to-noise ratios of the recordings.

If the yield of separable units per recording is based on setting some maximal permissible error rate in classification, the neural network approach outperformed both template matching and linear discriminant analysis. Because the neural network training process is iterative, rather than analytical, and is based on minimizing error, it typically found solution states with lower error rates than the other methods. Provided the networks were adequately sized, the peak classification success rates for the two architectures were indistinguishable. However, the number of hidden layer nodes required to achieve maximum classifiability was approximately half for the individual experts approach than for the monolithic network. This carries an advantage for real-time implementation since the number of computations required for each waveform is directly proportional to the number of hidden layer nodes. Also, the number of iterations required for convergence was less for the individual experts approach than for the monolithic network, presumably because of less spatial cross-talk interference during training [16]. This may represent an advantage for updating and adapting the network weights should gradual changes occur in the shapes of the action potential profiles.

Template matching with Euclidean distance performs better at rejecting artifactual waveforms than either the neural network approach or windowing. This method is attractive because of its relative simplicity; training consists of simply computing a mean waveform for each unit. Additionally, it is not necessary to retrain the whole system should new units appear and the method should exhibit good rejection of units that appear in a recording but were not included in the training set. On the other hand, the number of computational cycles required for template matching depends on the number of units present in the recording and is greater than that required for our neural network architecture when more than three or four units are present in a recording.

The most important criterion for neuroprosthetic applications is the number of reliable individual channels of information available from a single implant. The data presented here show that dual channel electrodes are clearly superior in this respect. The extent to which sensitivity to corruption by artifact is problematic for such applications remains to be determined, but neural network architectures that generate closed classification boundaries may offer improved artifact rejection while maintaining high classification performance [17].

ACKNOWLEDGMENT

The authors acknowledge the access to computer facilities granted by the University of Utah Supercomputing Institute.

REFERENCES

[1] E. V. Goodall, K. W. Horch, T. G. McNaughton and C. M. Lybbert, "Analysis of single-unit firing patterns in multi-unit intrafascicular recordings," *Med. & Biol. Eng. & Comput.*, vol. 31, pp. 257–267, 1993.

[2] B. C. Wheeler and W. J. Heetderks, "A comparison of techniques for classification of multiple neural signals," *IEEE Trans. Biomed. Eng.*, vol. BME-29, pp. 752–759, 1982.

[3] E. M. Schmidt, "Computer separation of multi-unit neuroelectric data: A review," *J. Neurosci. Meth.*, vol. 12, pp. 95–111, 1984.

[4] B. L. McNaughton, J. O'Keefe and C. A. Barnes, "The stereotrode: A new technique for simultaneous isolation of several single units in the central nervous system from multiple unit records," *J. Neurosci. Meth.*, vol. 8, pp. 391–397, 1983.

[5] I. N. Bankman, K. O. Johnson and W. Schneider, "Optimal recognition of neural waveforms," in *Proc. 13th Annu. Int. Conf. IEEE Eng. Med. Soc.*, vol. 1. Orlando, FL: 1991, pp. 409–410.

[6] E. V. Goodall and K. W. Horch, "Separation of action potentials in multi-unit intrafascicular recordings," *IEEE Trans. Biomed. Eng.*, vol. 39, pp. 289–295, 1992.
[7] K. Mirfakhraei and K. Horch, "Classification of action potentials in multi-unit intrafascicular recordings using neural network pattern recognition techniques," *IEEE Trans. Biomed. Eng.*, vol. 41, pp. 89–91, 1994.
[8] K. Potje-Kamloth, J. Janata and M. Josowicz, "Electrochemically prepared insulation for carbon fiber microelectrodes," *Ber. Bunsenges. Phys. Chem.*, vol. 93, pp. 1480–1485, 1989.
[9] T. Lefurge, E. Goodall, K. Horch, L. Stensaas and A. Schoenberg, "Chronically implanted intrafascicular recording electrodes," *Ann. Biomed. Eng.*, vol. 19, pp. 197–207, 1991.
[10] E. V. Goodall, T. M. Lefurge and K. W. Horch, "Information contained in sensory nerve recordings made with intrafascicular electrodes," *IEEE Trans. Biomed. Eng.*, vol. 38 pp. 846–850, 1991.
[11] R. O. Duda and P. E. Hart, "Pattern Classification and Scene Analysis," 1st ed. New York: Wiley & Sons, 1973.
[12] D. E. Rumelhart, G. E. Hinton and R. J. Williams, "Learning internal representattions by error propagation," in *Parallel Distributed Processing*, Rumelhart and McClelland, Eds. Cambridge MA: MIT Press, 1986, pp. 318–362.
[13] J.-B. Donnet and R. C. Bansal, *Carbon Fibers*, 2nd. ed. New York: Marcel Dekker, 1990.
[14] A. J. M. Starrenburg and G. C. Burger, "Carbon fiber as an electrode material," *IEEE Trans. Biomed. Eng.*, vol. 29, pp. 352–355, 1993.
[15] M. Malagodi, K. W. Horch and A. A. Schoenberg, "An intrasfascicular electrode for recording of action potentials in peripheral nerves," *Ann. Biomed. Eng.*, vol. 17, pp. 397–410, 1989.
[16] R. A. Jacobs, M. I. Jordan, S. J. Nowlan and G. E. Hinton, "Adaptive mixtures of local experts," *Neural Computation*, vol. 3, pp. 79–87, 1991.
[17] I. N. Bankman, J. Sadowsky and V. G. Sigillito, "A neural network for generating diverse decision boundaries with a minimal number of parameters," in *Proc. 14th Annu. Int. Conf. IEEE Eng. Med. Biol. Soc.*, vol. 3. Paris, France: 1992, pp. 1039–1041.

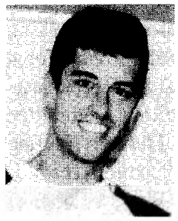

Timothy G. McNaughton (S'91) was born in Eglin, Forida in 1965. He received the B.S. degree in engineering from Harvey Mudd College, Claremont, California in 1988. He is currently a doctoral candidate in bioengineering at the University of Utah and a consultant at the Utah Supercomputing Institute. His research program focuses on optimizing materials and methods for extracting information from peripheral nerves using intrafascicular electrodes.

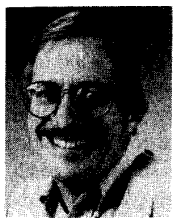

Kenneth W. Horch (M'88) received undergraduate and graduate degrees from Lehigh and Yale Universities, respectively.

He is currently Professor and Associate Chairman of Bioengineering and Professor of Physiology at the University of Utah. His research activities involve neuroprosthetics, sensory neurophysiology, motor control, and nerve repair and regeneration.

Dr. Horch is an active member of the Biomedical Engineering Society, the IEEE Engineering in Medicine and Biology Society, the Sunderland Society, and Sigma Xi.